I&EC research
Industrial & Engineering Chemistry Research

pubs.acs.org/IECR
Article

From CO_2 to Jet Fuel: Techno-Economic and Life-Cycle Assessment

Published as part of Industrial & Engineering Chemistry Research special issue "Advances in the Optimization of Process Operations-In Memory of Pedro Castro".

Marcelino Artur L. Fernandes, Frederico S. Coelho, Rita M. Martinho, Mariana G. Domingos, and Fernando G. Martins*

Cite This: *Ind. Eng. Chem. Res.* 2025, 64, 22321−22335

ABSTRACT: This work investigates the advantages of recycling and introducing reforming stages to enhance jet fuel production in a Power-to-Liquid (PtL) process while reducing direct air emissions. A flue gas stream containing 8%$_{vol}$ of CO_2 is considered, being the CO_2 captured via amine scrubbing units, and converted to jet fuel via a reverse water gas shift reaction, followed by a Fischer−Tropsch synthesis, and separated in an Atmospheric Crude Distillation Unit (ACDU). Three production scenarios are considered: the *Base* scenario, where CO_2 is not recycled within the process; the *Recycle* scenario, which separates and recycles unreacted CO_2 and H_2 to the reverse water gas shift reactor, via amine scrubbing systems and pressure swing adsorption; and the *Recycle + Reforming* scenario, which, in addition to CO_2 recycling, also converts unreacted hydrocarbon to syngas in a reforming reactor to be added to the Fischer−Tropsch reactor. Aspen Plus V12.1 is used for simulating the proposed scenarios, and the results are used to estimate the levelized costs of fuel and to perform the Life Cycle Assessments. The median values of the jet fuel production cost obtained in the *Recycle* and *Recycle + Reforming* scenarios are about half of that obtained in the *Base* scenario and very similar to each other, 2.7−3.7 €/L, and 2.7−3.6 €/L, respectively. The lowest bound of the range is in line with the available projections for jet fuel prices but is highly dependent on the selling of byproducts, such as electricity, steam, Liquefied Petroleum Gas (LPG), naphtha, and diesel, particularly for the *Recycle* case. Despite the increase in water and mineral resources use, these solutions reduce jet fuel Global Warming Potential (GWP), ranging from 27 to 59 gCO_2eq/MJ with system expansion, or about 37 gCO_2eq/MJ with energy allocation and assuming that green H_2 production impacts are zero. Using renewable energy-powered electricity would be enough to decrease the footprint to levels lower than 28.2 gCO_2eq/MJ, thus complying with the 70% emissions saving criterion established for renewable transport fuels of nonbiological origin in the European Union.

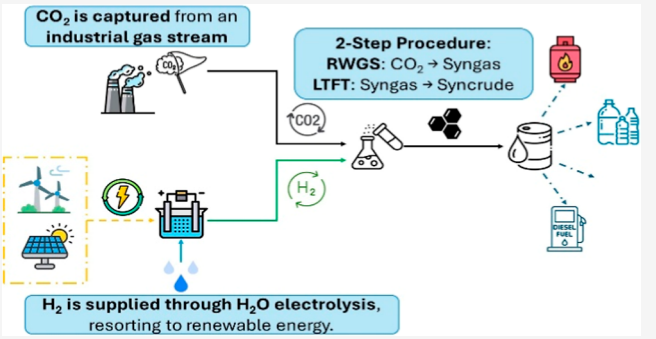

1. INTRODUCTION

Synthetic fuels have emerged as a promising alternative to fossil crude oil, whose reserves are projected to be depleted within approximately 40 years if current consumption trends persist.[1] With global oil demand expected to peak by 2028, accompanied by a 6% increase,[2] the production of synthetic fuels offers a viable pathway to reduce reliance on fossil resources. These fuels present several advantages: they are chemically compatible with existing infrastructure, exhibit cleaner combustion due to the absence of sulfur and particulate matter,[3] and when produced through CO_2 utilization, enable the valorization of emissions that would otherwise be released into the atmosphere. Moreover, when deployed before 2040, synthetic fuels produced from captured CO_2 offer a strategic emissions reduction option for sectors regulated under the EU Emissions Trading System (EU ETS).[4] This provides a transitional mitigation pathway while alternative technologies (such as Carbon Capture and Storage (CCS), fuel switching, and hydrogen) continue to scale. The relevance is particularly high for hard-to-abate sectors such as cement and glass, where decarbonization is progressing more slowly due to technical constraints.

The importance of synthetic fuels is reflected in recent policy developments. The International Energy Agency (IEA) estimates that 7 million tonnes of CO_2 should be utilized annually for synthetic fuel production to align with Net Zero

Received: August 6, 2025
Revised: October 31, 2025
Accepted: November 3, 2025
Published: November 11, 2025

https://doi.org/10.1021/acs.iecr.5c03132
Ind. Eng. Chem. Res. 2025, 64, 22321−22335

targets by 2030.[5] Furthermore, the European Union's ReFuelEU Aviation regulation mandates that synthetic aviation fuels derived from renewable hydrogen and captured carbon must reach a 35% share of all fuel used in EU airports by 2050.[6]

Within the family of power-to-liquid (PtL) processes (where CO_2 is converted to liquid fuels using hydrogen derived from electrolysis), long-chain hydrocarbons have attracted increasing attention. Compared to other PtL products like methanol (MeOH) and dimethyl ether (DME), synthetic hydrocarbons (e.g., synthetic crude and jet fuel) are expected to experience the highest market growth, particularly in aviation, with a projected Compound Annual Growth Rate (CAGR) of 14.3% from 2023 to 2033.[7−9]

This study focuses on the production of synthetic hydrocarbons via the Reverse Water−Gas Shift (RWGS) reaction, which converts CO_2 and H_2 into carbon monoxide (CO). The resulting CO then reacts with H_2 in a Fischer−Tropsch (FT) synthesis to produce synthetic hydrocarbons in the form of synthetic crude.

While there has been increasing research into PtL systems converting CO_2 into hydrocarbons, previous works have focused on (1) the direct conversion of CO_2 into hydrocarbons[10] and its comparison with indirect pathways,[11−13] (2) comparisons between PtL versus PtL and SNG (synthetic natural gas) systems,[12−14] (3) the configuration of the system downstream of the FT reactor and prior to refinement,[15] (4) different hydrogen production routes (alkaline electrolysis and solid oxide electrolysis) prior to RWGS or coelectrolysis of CO_2 and H_2,[16,17] and (5) the influence of operational conditions.[15,18] These studies consistently identify hydrogen as the primary cost driver[19,20] yet cost estimates for jet fuel remain widely dispersed, ranging from 0.50 €/L to 14.90 €/L, due to differences in methodological approaches and system configurations (Figure 1).

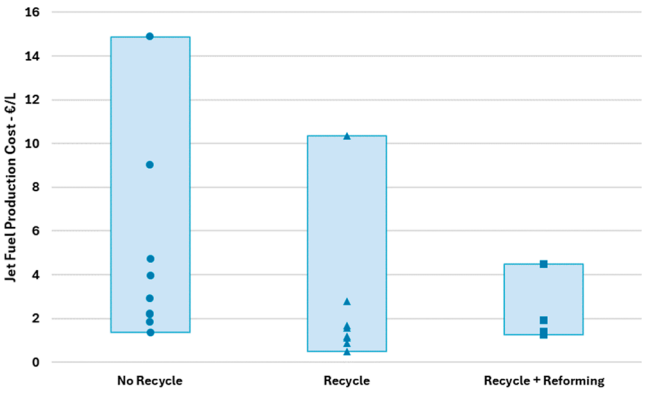

Figure 1. −Retrieved costs for jet fuel production, based on literature reports (circle, triangular, and squared points represent the individual retrieved points).

Among these design variables, the use of recycling streams, whether through the recirculation of unreacted CO_2 and H_2 from the RWGS and FT stages or through the reforming of FT off-gases, varies significantly. Figure 1 illustrates the cost ranges for cases without recycling, with unreacted gas recycling, and with FT off-gas reforming. The individual data points represent values which are reported in the literature.[10−13,16−18,20−26] However, a direct side-by-side comparison of these configurations under consistent boundary conditions is lacking in the literature.

This work addresses this gap by systematically evaluating three PtL scenarios: (1) a base case without gas recycling; (2) a recycling case, where unreacted CO_2 and H_2 are recirculated; and (3) a recycling plus reforming case, where a fraction of the FT off-gas is also reformed to recover additional syngas (a mixture of CO and H_2).

In addition to this comparative approach, three further contributions enhance the depth of the analysis. First, this work considers the composition of a flue gas stream from a hard-to-abate sector, i.e., a flue gas stream from the glass industry, and includes the equipment required for its separation into a CO_2 stream. Second, a kinetic model is employed for FT synthesis that dynamically adjusts the chain growth probability (α) based on process conditions, enabling a more accurate simulation of product yields. Third, an Atmospheric Crude Distillation Unit (ACDU) is incorporated into the model to reflect a realistic postprocessing step, allowing refined assessment of jet fuel production quantities and stream compositions.

The economic and environmental performance of the three PtL configurations is assessed using a Techno-Economic Analysis (TEA) to estimate the cost per liter of jet fuel, a Life Cycle Assessment (LCA) to evaluate the impact on greenhouse gas (GHG) emissions and resource scarcity, and a regulatory GHG emissions calculation, based on EU guidelines, which evaluates whether the jet fuel produced meets the criteria to be classified as a sustainable fuel under the renewable energy directive. Together, these assessments aim to provide a robust assessment of design choices in synthetic fuel production, supporting more informed decisions on process optimization and technology deployment under industrially relevant conditions.

2. CASE STUDY AND PRODUCTION SCENARIOS

This work considers a 34,000 N $m^3 \cdot h^{-1}$ flue gas stream with 8%$_{vol}$ of CO_2, 8%$_{vol}$ oxygen (O_2), 3%$_{vol}$ water (H_2O), and the balance being N_2. This is the typical composition of a flue gas from a glass industry (after removal of contaminants, such as NO_x, SO_x, and particles), and nearly 47% of European glass producers with verified emissions in 2023 have point source emissions of this scale or above.[4]

The CO_2 present in a flue gas stream is captured with an amine scrubbing process and is converted into liquid fuels (e.g., jet fuel, LPG, naphtha, and diesel) via a Reverse Water Gas Shift (RWGS) reaction with green H_2, i.e., H_2 produced by electrolysis using renewable energy sources, followed by Fischer−Tropsch synthesis. The simplified Process Flow Diagrams (PFD) for the three production scenarios are shown in Figure 2.

2.1. *Base* Scenario. The CO_2 is captured from the flue gas through chemical absorption using Monoethanolamine (MEA) as a solvent. The capture rate is fixed at 90%, resulting in a CO_2 stream of 5 ton$\cdot h^{-1}$. After capture, the CO_2 is mixed with green H_2 at high temperature to favor the RWGS reaction. The reactor outlet is then cooled to condense and separate most of the produced H_2O from the gas stream. This dry gas stream is subsequently reheated to meet the operating conditions of the FT reaction. After the FT reactor, the outlet stream is cooled to enable a vapor−liquid−liquid separation. The resulting gas stream is used as fuel in a furnace, supplying the heat required by the RWGS reactor, while the organic phase is partially

https://doi.org/10.1021/acs.iecr.5c03132
Ind. Eng. Chem. Res. 2025, 64, 22321−22335

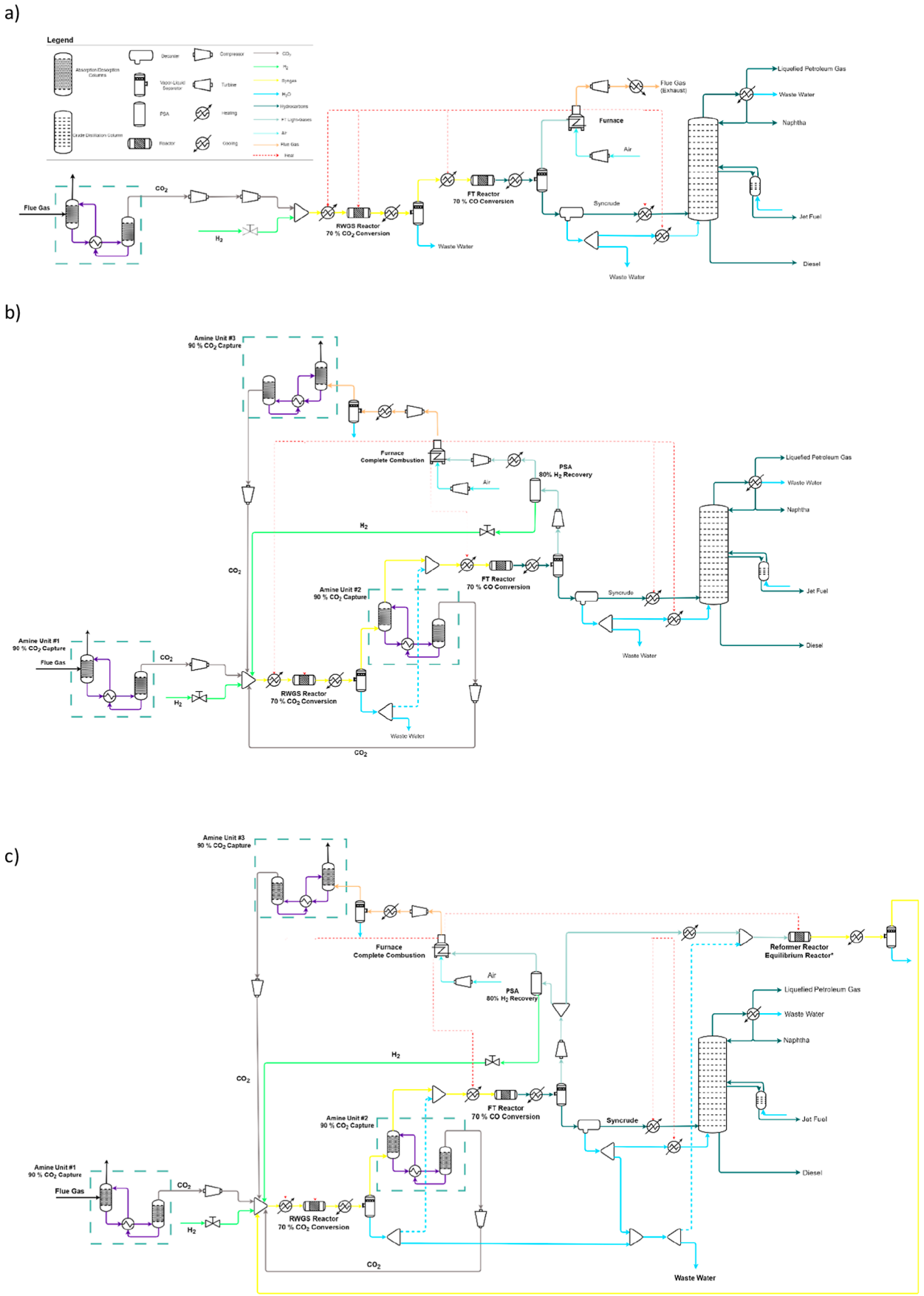

Figure 2. PFD of (a) *base* scenario; (b) *recycle* scenario; and (c) *recycle* + *reforming* scenario.

https://doi.org/10.1021/acs.iecr.5c03132
Ind. Eng. Chem. Res. 2025, 64, 22321−22335

vaporized and sent to an Atmospheric Crude Distillation Unit (ACDU).

2.2. *Recycle* Scenario. In the *Recycle* scenario, four modifications have been implemented: (1) introduction of a CO_2 capture unit after the RWGS reaction—under the established operating conditions, the reactor outlet stream contains approximately 22%$_{vol}$ H_2O and 9%$_{vol}$ CO_2. These components are removed before entering the FT reactor: H_2O is separated in a vapor—liquid separator by cooling, and CO_2 is captured in an amine scrubbing unit, with a 90% capture rate. Removing CO_2 increases the partial pressure of the FT reactants (CO and H_2), thereby reducing the catalyst requirements in the FT reactor. The captured CO_2 is recycled to the beginning of the process, increasing syngas and thus jet fuel production; (2) installation of a Pressure Swing Adsorption (PSA) unit after the FT reactor to recover part of the unreacted H_2, thus reducing the demand for fresh green H_2. The gas stream, from the vapor—liquid—liquid separation, contains approximately 63%$_{vol}$ of H_2. The separation is modeled on Aspen Plus, assuming an 80% recovery of pure H_2, an approach based on the work of Mivechian and Pakizeh.;[27] (3) use of the PSA purge stream as a fuel in the furnace. The excess heat released from the furnace, together with the heat generated in the FT reactor, must be sufficient to supply the reboilers in the stripping sections of the three amine scrubbing units used in the process (Amine Units #1, #2, and #3 in Figure 2); (4) capture of CO_2 from the furnace flue gas in a second amine scrubbing unit operating at 90% capture efficiency. The recovered CO_2 is also recycled to the beginning of the process.

2.3. *Recycle* + *Reforming* Scenario. This scenario is an extension of the *Recycle* scenario, in which a portion of the light gas products from the FT reaction is directed to a reforming reactor to increase the production of syngas for reuse within the process. The steam required for the reforming section is supplied by H_2O recovered throughout the process. With the introduction of the reforming step, the duty of the furnace is set to be greater than or equal to the sum of the duties of the RWGS and the reforming reaction. The heat of the FT reaction, and any excess heat from the furnace, must also be sufficient to provide heat to the reboilers of the CO_2 capture units within the process (Amine Units #1, #2, and #3) in Figure 2.

3. MODELING AND PROCESS SIMULATION

The three production scenarios were simulated using Aspen Plus V12.1. The Peng—Robinson (PENG-ROB) thermodynamic package was applied to the overall processes, while the Electrolyte Non-Random Two-Liquid with the Redlich—Kwong Equation of State (ENRTL-RK) was used for the amine scrubbing units. Aspen Energy Analyzer V12.1 was also employed to develop the heat integration schemes.

3.1. CO_2 Capture—Amine Scrubbing. In this work, CO_2 is captured from the flue gas streams by using a chemical absorption process with MEA as the solvent. All amine scrubbing units were designed to achieve a CO_2 capture rate of 90%, operating at the 80% flooding limit in the columns. For the regeneration of the amines, the columns were configured to release all captured CO_2 by adjustment of the distillate flow rate. The kinetic model used in the simulations is based on the work of Luo et al.[28]

3.2. Water Electrolysis. The H_2O electrolysis process was modeled in Python using an in-house model developed at CoLAB Net4CO_2.[29] For the H_2 demand estimated for each scenario with Aspen Plus V12.1, the model determines the share of solar PV and wind energy required as well as the installed capacities for the hybrid renewable power plant and the H_2 storage facilities, which guarantee a continuous supply of H_2 at the lowest cost for a given electrolyzer capacity. The capacity factors for the hybrid renewable plant are derived from historical data of the Portuguese electricity system,[29] thereby incorporating a regional perspective into the case study.

3.3. RWGS Reactor. The reactions considered within the RWGS reactor are shown in Table 1.

Table 1. Main Reactions Considered for the RWGS System

RWGS	$CO_2 + H_2 \leftrightarrow CO + H_2O$	(1)	1
CO methanation	$CO + 3H_2 \leftrightarrow CH_4 + H_2O$	(2)	2
CO_2 methanation	$CO_2 + 4H_2 \leftrightarrow CH_4 + 2H_2O$	(3)	3

A *RPlug* reactor block was used to model this reaction, using the kinetic model developed by Vidal Vázquez et al.[30] for a Ni/Al_2O_3 catalyst, with 2%$_{wt}$ in nickel. Once the kinetic model was validated with the reported values, the operational conditions were set at 900 °C and 20 bar to achieve a CO_2 conversion of 70%, while maintaining a pressure slightly above that of the FT reaction (19.5 bar), thus eliminating the need for intermediate compression stages.

For all scenarios, a target molar H_2/CO ratio of 2.15 at the FT reactor inlet was selected. In the *Base* and *Recycle* scenarios, this ratio is achieved with a feed molar H_2/CO_2 ratio of 2.3. In the *Recycle* + *Reforming* scenario, the H_2/CO_2 ratio is determined based on design specifications, as the reforming section generates additional syngas, which is then fed to the RWGS reactor. The heat required to operate this reactor isothermally is supplied by a furnace.

3.4. FT Synthesis. The Fischer—Tropsch (FT) synthesis is an exothermic polymerization process that occurs at pressures close to 20 bar, yielding various types of hydrocarbons, including paraffins, olefins, and alcohols. Table 2 lists the main chemical reactions present during the Fischer—Tropsch synthesis, where n is the number of carbon atoms present in a given hydrocarbon.[31]

Table 2. —Main Chemical Reactions in the Fischer—Tropsch Synthesis

paraffins	$nCO + (2n+1)H_2 \leftrightarrow C_nH_{2n+2} + nH_2O$	(4)	4
olefins	$nCO + (2n)H_2 \leftrightarrow C_nH_{2n} + nH_2O$	(5)	5
alcohols	$nCO + (2n)H_2 \leftrightarrow C_nH_{2n+2}O + (n-1)H_2O$	(6)	6

This work considers Low-Temperature Fischer—Tropsch (LTFT) conditions, typically occurring under a cobalt-based catalyst and operating temperatures between 190 and 250 °C. Under these conditions, the product mainly consists of linear paraffins and light olefins, with minimal to no activity toward the WGS reaction. The kinetic model developed by Pandey et al.[32] was employed after its validation with the reported values, which uses a 20%Co/0.5Re γ-Al_2O_3 catalyst, as it accounts for deviations from the Anderson-Schultz-Flory (ASF) distribution, particularly in the C_1 and C_2 fractions, and is applicable to hydrocarbons of any chain length, eliminating the need for a

https://doi.org/10.1021/acs.iecr.5c03132
Ind. Eng. Chem. Res. 2025, 64, 22321—22335

predefined cutoff for high-carbon-number products or the creation of a lumped representative component.[10,12,13] The general reactions implemented in the model for paraffin and olefin production are listed in Table 3.

Table 3. Generic Reaction Implemented in the Kinetic Model to Model Paraffin and Olefin Production

paraffin	$CO + UH_2 \leftrightarrow \vartheta_n C_n H_{2n+2} + H_2O$	(7)	7
olefins	$CO + U'H_2 \leftrightarrow \vartheta'_n C_n H_{2n} + H_2O$	(8)	8

In eqs 7 and 8, U and ϑ_n represent the stoichiometric coefficients of the reactions for hydrogen and the hydrocarbons, respectively. Considering the implemented kinetic model, these coefficients are calculated by two model-specific parameters: the chain-growth probability, α, and the distribution parameter, β. Larger values of α and β correspond to an increased production of heavier hydrocarbons and olefinic compounds, respectively. These parameters are dependent on the operating conditions, namely, temperature and the partial pressures of H_2O and CO.

To implement this model, the "Custom" kinetic option of Aspen Plus was used, enabling dynamic updates of the parameters according to varying operating conditions, which is especially important in scenarios involving recycle streams. The model accounts for paraffinic and olefinic compounds up to C_{30}, ensuring that the mass lost in the reactor remains below 5% across all scenarios. To achieve paraffinic mass balance closure within an error of 10^{-5}, the hydrocarbon length would need to be extended to C_{57} for the *Base* scenario, and C_{74} for both the *Recycle* and the *Recycle + Reforming* scenarios. However, extending the hydrocarbon range significantly increases computational demand and would also require adding hydrocarbons to the Aspen Plus simulation, which are not part of the database, thereby introducing additional uncertainty in thermodynamic property estimations.

The reactor pressure was fixed at 19.5 bar, and an isothermal operation at 250 °C was assumed. This high temperature slightly hinders the production of heavier hydrocarbons. However, by increasing the molar fraction of H_2O to 3.25% by reintroducing a small amount of H_2O separated from the RWGS outlet stream, an increase in α was observed, accompanied by a sharp decrease in β, therefore favoring the production of heavier paraffinic hydrocarbons.

The heat released by the reaction can be used in two distinct ways: the first one is the direct integration with the CO_2 capture units, most specifically with the reboilers in the regeneration column; otherwise, the heat can be used to generate steam to either be sold or used in the process.

3.5. Atmospheric Crude Distillation Unit. At the Atmospheric Crude Distillation Unit (ACDU), the syncrude is split into different fractions or "cuts" (e.g., naphtha and jet fuel), which consist of narrower hydrocarbon product distributions.

In terms of design, the distillation column was composed of 30 stages, being fed, at the bottom, by steam at 160 °C and 4 bar generated using heat released in the FT reaction, to remove the lighter hydrocarbons from the liquid streams.[33] The syncrude is partially vaporized at 260 °C, being fed in stage 24. A partial condenser, operating at 30 °C, also exists to separate the naphtha cut, the decant-water stream, and the light end, here designated by Liquefied Petroleum Gas (LPG). In addition, the unit contains one side stripper, designed to extract the jet fuel cut, with the liquid being withdrawn at the 16th stage. The vapor flow exiting from the side stripper is reintroduced in the main distillation column at the 14th stage. The distillate rate of the main column, as well as the bottom flow rate of the side stripper, was set based on column design specifications using ASTM D86 temperatures at 95% distillate (volume) for naphtha or jet fuel as quality parameters.

While the actual refining process is highly complex and involves numerous steps, for this initial approach, it is assumed that the outlet streams of the ACDU are ready-to-sell products, albeit possibly containing some impurities or not meeting the standards related to some properties. Thus, this unit considers the following main product streams: (i) Liquefied Petroleum Gas (LPG), which is mostly comprised of hydrocarbons between C_2−C_4; (ii) naphtha, corresponding to hydrocarbons between C_4−C_{11}; (iii) jet fuel, having hydrocarbons between C_{11}−C_{14}; and (iv) diesel, with the hydrocarbons above C_{14+}.

3.6. Reforming Reactor. The reforming reaction produces CO and H_2 from different hydrocarbons. The most common reforming reaction is the Steam Methane Reforming (SMR)−eq 9, which typically operates between 700−1000 °C and 15−50 bar.[34]

$$\text{SMR Reaction}\quad CH_4 + H_2O \rightarrow CO + 3H_2 \tag{9}$$

Although there are reports of kinetic models for the SMR reaction, models for the reforming of heavier hydrocarbons are scarce. In this work, the reforming stage was simulated using an *RGibbs* equilibrium reactor. This approach is considered a reasonable approximation due to the high reaction rates typically observed in the SMR reaction, which suggests that the system operates near equilibrium at elevated temperatures.[35] The reactor was established to operate at 860 °C and 20 bar to avoid any intermediate compression, and the molar feed ratio of H_2O/CH_4 was set to 5.5.

3.7. Furnace. The furnace supplied heat for the RWGS and the SMR reactors. In the *Recycle* and the *Recycle + Reforming* scenarios, the generated flue gas is reused by removing the CO_2 from the stream. The furnace was simulated by using an *RGibbs* equilibrium reactor operating adiabatically at 10.6 bar. In all simulated scenarios, the resulting flue gas is expanded to 2 bar to generate electricity for use within the process. This expansion enables the *Base* scenario to be self-sufficient in terms of electricity. Although self-sufficiency is not achieved in the other scenarios, the same expansion step was applied for consistency across all cases and to ensure compatibility with downstream units, such as the amine scrubbing systems. In Table 4, the required electricity and the generated electricity from the turbine are quantified for each of the scenarios.

Table 4. −Required Electricity and Generated Electricity from the Turbine in Each Scenario[a]

	required electricity (kWh)	turbine (kWh)
base	1490	1490
recycle	2900	1485
recycle + reforming	1680	381

[a]The temperatures of the flue gas streams after expansion are 400 °C for the *Base* and 150 °C for the *Recycle* and *Recycle + Reforming* scenarios. Using these levels of temperature to generate steam for additional revenues has been considered.

https://doi.org/10.1021/acs.iecr.5c03132
Ind. Eng. Chem. Res. 2025, 64, 22321−22335

4. PROCESS RESULTS

4.1. Product Distribution. To evaluate and compare the performance of synthetic fuel production scenarios, two FT reaction-specific parameters must be analyzed: the chain growth probability, α, and the relative amount of olefinic compounds, β. The values obtained for the different scenarios are presented in Table 5, and a graphical representation of the α values is shown in Figure 3.

Table 5. FT Specific Parameters for the Different Scenarios

	base	*recycle*	*recycle + reforming*
α	0.80	0.84	0.84
β	0.67	0.69	0.69

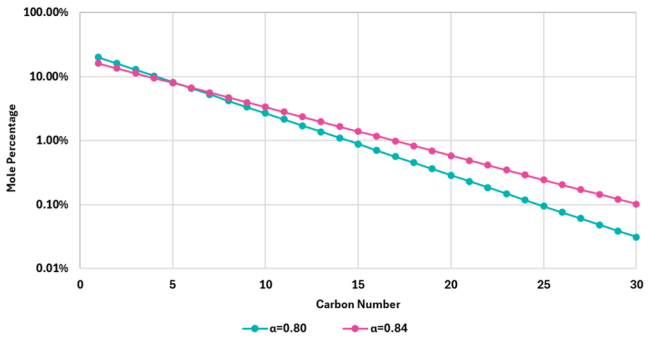

Figure 3. Ideal ASF distribution for the obtained α values.

While the absolute differences in α and β may appear small, an α value of 0.84 results in a molar fraction of the heavier hydrocarbons that is nearly 1 order of magnitude higher than that observed for an α of 0.80. This increase in α for the scenarios with CO_2 recycling is primarily attributed to the small amount of H_2O introduced into the FT reactor. This effect has been previously reported [43]; however, the amount of added H_2O should be carefully controlled to avoid permanent catalyst deactivation.[36]

4.2. Carbon Efficiency. Carbon Efficiency (CEF) is used to quantify the amount of carbon that is effectively retained in the products and is calculated using the following equation

$$\mathrm{CEF} = \frac{\sum C_{\mathrm{Product}}}{\sum C_{\mathrm{In}}} \tag{10}$$

where C_{Product} stands for the number of carbon moles present in all products (jet fuel or any side products), while C_{In} represents the amount of fresh carbon fed to the process after the CO_2 capture from the flue gas.

Furthermore, the obtained reaction conversion and the Weight Hourly Space Velocity (WHSV) in the different kinetically driven reactions within the process were quantified, with the obtained values shown in Table 6. As for the reforming reactor, the conversion is calculated in relation to the sum of the mass of the whole range of hydrocarbons in the feed and to the sum of the mass of the whole range of hydrocarbons in the reactor outlet.

Table 6. Carbon Efficiency for the Different Scenarios

	base	*recycle*	*recycle + reforming*
CEF (%)	30.0	85.2	90.7
RWGS CO_2 conversion (%)	70		
RWGS WHSV (h^{-1})	3120	2844	3413
FT CO conversion (%)	70		
FT WHSV (h^{-1})	24.1	15.5	16.0
reforming conversion (%)			52

As shown in Table 6, the introduction of CO_2 recycle streams significantly increases the CEF, nearly tripling it from the *Base* to *Recycle* scenarios. The addition of the reforming section further improves the CEF, resulting in an increase of 5.5% compared to the *Recycle* scenario.

4.3. Process Metrics Analysis. Tables 7 and 8 present the process inputs and outputs for the three scenarios. Inputs include raw materials (CO_2 and H_2), catalysts, and utilities (cooling water and electricity). The reforming catalyst is not included, as its cost—being Nickel-based—is not expected to be significant. Outputs consist of different crude oil cuts and steam. Both absolute and specific values (per liter of jet fuel) are presented, with the specific values referring to the absolute amounts normalized by the liter of jet fuel produced. Regarding the catalysts, the specific consumption is not calculated since it does not have any physical significance.

All scenarios are self-sufficient in terms of heat, highlighting the relevance of heat integration in this process. As a result, the utilities are limited to cooling water and electricity; see Table 7.

For the same amount of CO_2 fed into the process, the *Base* scenario requires less utilities, catalyst, and H_2 compared to the *Recycle* and *Recycle + Reforming* scenarios, e.g., the *Base* scenario consumes approximately 7 and 4.5 times less cooling water than the *Recycle* and the *Recycle + Reforming* scenarios, respectively. This is mainly due to the smaller scale of the process in the absence of recycle streams. Additionally, the *Base* scenario is more productive in terms of steam generation, as less heat is needed for the regeneration in the amine scrubbing units since CO_2 is only captured from the flue gas at the process inlet.

Scenarios that incorporate CO_2 recycling streams show clear advantages in terms of jet fuel production. The *Recycle* scenario produces nearly 3 times more jet fuel than the *Base* scenario, using the same amount of fresh CO_2 feed. The *Recycle + Reforming* scenario is only 7% more productive in jet fuel compared to the *Recycle* scenario.

The increase in jet fuel production in the *Recycle* and *Recycle + Reforming* scenarios leads to a lower specific consumption of H_2 and cooling water compared to the *Base* scenario. Specific diesel production is almost 60% larger. The *Base* scenario only outperforms the others in being electrically self-sufficient and in generating significantly more specific steam, i.e., over 1.7 times more than the *Recycle* scenario and 16 times more than the *Recycle + Reforming*. In the *Recycle + Reforming* scenario the amount of available steam is lower than in the *Recycle* scenario, as a portion of the generated steam is used internally in the reforming process, resulting in a 23% reduction in the specific fresh H_2 consumption. These are the two main differences between these alternative scenarios.

5. TECHNO-ECONOMIC ANALYSIS (TEA)

The techno-economic analysis included Capital Expenditure (CAPEX), Operation Expenditure (OPEX), and revenues. For the CAPEX, all process units were considered.

Equipment costs were obtained using Aspen Process Economic Analyzer V12 (APEA) for all process equipment, except for the RWGS reactor, FT reactor, PSA unit, and heat exchangers. The cost of the RWGS reactor was estimated

https://doi.org/10.1021/acs.iecr.5c03132
Ind. Eng. Chem. Res. 2025, 64, 22321−22335

Table 7. Process Inputs for the *Base*, *Recycle*, and *Recycle + Reforming* Scenarios[b]

	base		*recycle*		*recycle + reforming*	
	absolute consumption	specific consumption	absolute consumption	specific consumption	absolute consumption	specific consumption
CO_2 (ton·h^{-1})|(kg·L^{-1})[a]>	5.0	11.7	5.0	4.40	5.0	4.14
H_2 (ton·h^{-1})|(kg·L^{-1})	0.5	1.23	1.0	0.92	0.9	0.71
RWGS catalyst (kg)	1.8		4.8		3.7	
FT catalyst (ton)	0.2		0.4		0.5	
cooling water (ton·h^{-1})|(ton·L^{-1})	9.7×10^2	2.27	2.5×10^3	2.19	1.8×10^3	1.49
electricity (MWh)|(kJ·L^{-1})			0.9	0.8	1.7	1.1

[a]The second units correspond to the specific consumption. [b]"Specific Consumption" refers to the absolute amount normalized by the volume (liters) of jet fuel produced.

Table 8. Process Outputs for the *Base*, *Recycle*, and *Recycle + Reforming* Scenarios[a]

	base			*recycle*			*recycle + reforming*		
	absolute production	specific production	LHV	absolute production	specific production	LHV	absolute production	specific production	LHV
steam (ton·h^{-1})|(kg·L^{-1})	8.1	19.0	2.8	4.7	4.1	2.8	0.5	0.45	2.8
LPG (L·h^{-1})|(−)	15	3.45×10^{-2}	32.9	28	2.44×10^{-2}	39.8	28	2.35×10^{-2}	41.0
naphtha (kg•h^{-1})|(kg•L^{-1})	1.2×10^2	0.42	45.1	2.8×10^2	0.16	45.2	3.0×10^2	0.37	45.3
jet fuel L·h^{-1}	4.3×10^2	-	38.5	1.1×10^3	-	38.1	1.2×10^3	-	38.1
diesel (L·h^{-1})|(−)	1.2×10^2	0.29	42.6	5.5×10^2	0.48	42.6	5.6×10^2	0.46	42.6

[a]"Specific Production" refers to the absolute amount normalized by the volume (liters) of jet fuel produced. "LHV" refers to the lower heating value obtained for each stream, in MJ·kg^{-1}.

based on the heat duty required for the reaction, following the approach described in literature.[18] For the FT reactor, the cost was calculated using the standard volumetric flow rate of the reactor feed, as outlined in the work of Zang et al.[37] The PSA unit cost was estimated using the methodology described in the work of Mivechian et al.,[27] which considers similar operating conditions. For the heat exchangers, stream data were imported into the Aspen Exchanger Design & Rating V12 software (EDR) to enable detailed equipment sizing and cost estimation.

The OPEX included cooling water, catalysts for the FT and RWGS reactions (assuming both are replaced every 2 years), H_2, and electricity. Furthermore, all expenses related to the amine, either by its replacement, which was assumed to occur every 2 years, as well as the required makeup, were accounted for in the OPEX, with the reference cost for the amine being based on current market prices[38]

Reference prices for electricity were obtained from historical data,[39] based on a data set of 62 points. Estimates for the FT catalyst, RWGS catalyst, and naphtha prices were derived from historical data comprising 48, 16, and 36 points, respectively, as reported in literature.[40−42] For H_2, a case-specific cost distribution was generated using the model developed in the work of Rangel et al.,[43] which is described in Section 3.2.

The revenues accounted for the economic value of the outlet streams, namely, steam and various syncrude cuts. Their potential prices were assumed to vary uniformly, based on reference values from the literature.[44,45]

To estimate the final jet fuel production cost, the Monte Carlo method was applied to assess the uncertainty inherent to the process, using Oracle's Crystal Ball software.[46] This analysis provides various percentiles, with the most relevant being P10, P50, and P90, representing the jet fuel production cost with a 10%, 50%, and 90% confidence, respectively. For each input variable, the associated probability distribution was determined using Oracle's Crystal Ball "Fit Distribution to Data" feature. The specific parameters used, such as Location, Mean, and Standard Deviation for the log−normal distribution; Minimum, Maximum, Alpha, and Beta for the beta distribution; Minimum, Maximum, and Likeliest for the triangular distribution; Minimum and Maximum for the uniform distribution; and Likeliest and Scale for the minimum extreme distribution, are detailed in Table 9.

5.1. Results. For each scenario, two cases are considered.

- Case A: the generated byproducts (steam, LPG, naphtha, and diesel) are not included in the cost assessment; therefore, potential revenues from these streams are not accounted for;
- Case B: the generated byproducts (steam, LPG, naphtha, and diesel) are included in the cost assessment, and their revenues were taken into consideration.

For each scenario, 150,000 Monte Carlo runs were conducted. The resulting cost distributions were used to determine the P10, P50, and P90 values of the jet fuel production cost, as shown in Figure 4, with the limits of the box being the P10 and P90, and the data points representing the P50 for each case.

The introduction of CO_2 recycling is the main driver of cost reduction. Considering the P50 values for the scenarios where no revenues from byproducts are included, a 43−44% decrease in production cost is observed for both the *Recycle* and *Recycle + Reforming* scenarios. Similarly, accounting for revenues from byproducts further reduces the cost by 6% and 25%, with the highest relative decrease observed in the *Recycle* scenario.

To compare the production cost of jet fuel with that of conventional fuel, it is convenient to express the prices in €/L. Therefore, the lower heating value (LHV) of the produced jet fuel is used to convert the costs to the appropriate units. The LHVs for each simulation are presented in Table 10, and the corresponding statistical percentiles, in €/L, are shown in Figure 5.

https://doi.org/10.1021/acs.iecr.5c03132
Ind. Eng. Chem. Res. 2025, 64, 22321−22335

Table 9. Summary of the Assumed Distributions for the Monte Carlo Analysis

variable	distribution type	input parameters	units
total CAPEX	triangular	minimum value = 70% of obtained CAPEX, through APEA maximum value = 150% of obtained CAPEX, through APEA	M€
FT catalyst	lognormal	location = 25,500 mean = 43,150 Std. dev = 24,500	€/ton
RWGS catalyst	lognormal	location = 0 mean = 13,750 Std. dev. = 5550	€/ton
cooling water	triangular	minimum value = 0.0175 maximum value = 0.0375 likeliest value = 0.025	€/ton
MEA	uniform	minimum value = 1.5 maximum value = 2.5	€/kg
H_2 (*base*)	minimum extreme	likeliest = 5.19 scale = 1.03	€/kg
H_2 (*recycle*)	gamma	location = 2.02 scale = 0.64 shape = 2.71	€/kg
H_2 (*recycle + reforming*)	minimum extreme	likeliest = 4.92 scale = 0.97	€/kg
electricity	lognormal	location = 0.01 mean = 0.09 Std. Dev. = 0.07	€/kWh
LPG[44]	uniform	minimum value = 0.58 maximum value = 1.24	€/L
naphtha	beta	minimum = 0.06 maximum = 0.98 alpha = 2.92 beta = 2.37	€/kg
diesel[44]	uniform	minimum value = 1.05 maximum value = 2.02	€/L
steam	uniform	minimum value = 10 maximum value = 30	€/ton

Table 10. Jet Fuel LHV for the Different Simulations

	base	*recycle*	*recycle + reforming*
LHV−MJ/L	0.485	0.500	0.500

From Figure 5, it is possible to see that the *Recycle* and *Recycle + Reforming* scenarios are capable of producing jet fuel within the projected price of synthetic fuel production,[47] in 2050, which is comprehended between 1.16 and 2.66 €·L^{-1}. Table 11 presents the probability of each simulated scenario producing jet fuel within this range, based on the obtained probability function.

For scenarios involving recycling streams and accounting for byproduct revenues, there is over a 40% probability that the production cost falls within the projected fuel price range. However, this probability drops significantly, to below 15%, when no byproduct revenues are considered. The reduction is even more pronounced in the scenario without reforming, being, therefore, more dependent on the selling of byproducts. This was already expected, as the *Recycle + Reforming* scenario has a lower specific consumption of H_2. Indeed, the hydrogen price, which represents between 80 and 90% of the total cost of jet fuel production, depending on the cost, is also in line with some previously published works, as shown in Figure 6.

6. LIFE CYCLE ASSESSMENT (LCA)

To comprehensively assess the environmental performance of the studied CCU systems, two complementary methodologies are applied.

The first approach is product-focused and follows the methodology defined by the European Commission for calculating GHG emissions savings from recycled carbon fuels (see Figure 7). This framework[48] focuses exclusively on climate impacts and is applied to compare life-cycle GHG emissions of the jet fuel toward a fossil fuel benchmark of 94 gCO_2eq/MJ, with the purpose of verifying whether it complies with the regulatory threshold of achieving at least a 70% reduction for being classified as a sustainable recycled carbon fuel under the Renewable Energy Directive scope.

The second analysis is market-focused and consists of a Life Cycle Assessment (LCA) following ISO 14040:2006[49] and the guidelines from the Global CO_2 Initiative.[50] It aims to quantify the environmental impacts associated with the different scenarios and the marginal effect of substituting conventional

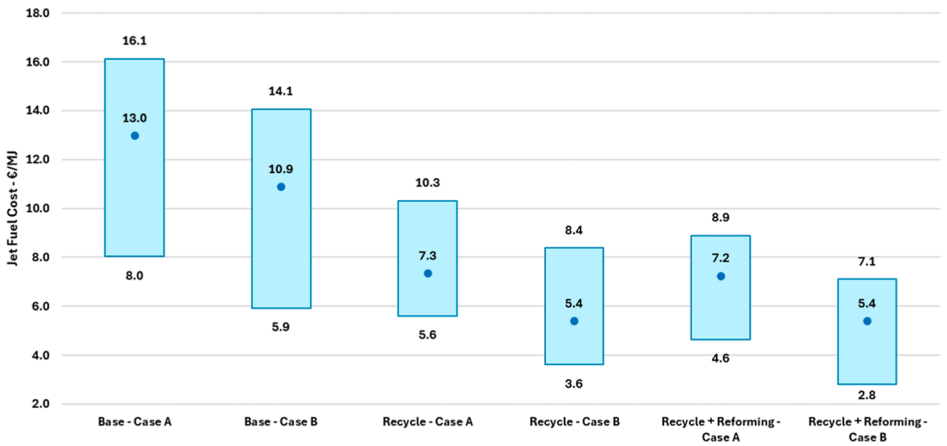

Figure 4. −Statistical Percentiles for the simulated scenarios, in €/MJ. Circular points represent the obtained P50 for each case, while the lower and higher boundaries of the boxes represent the P10 and P90 for each case, respectively.

https://doi.org/10.1021/acs.iecr.5c03132
Ind. Eng. Chem. Res. 2025, 64, 22321−22335

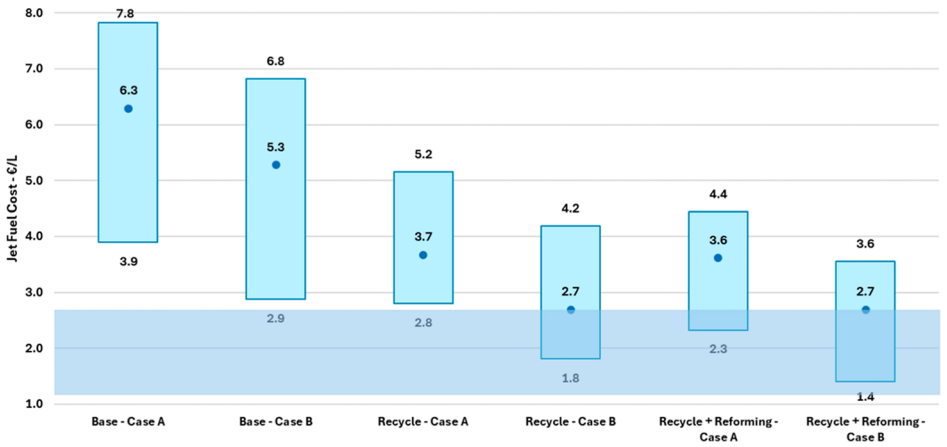

Figure 5. Statistical Percentiles for the simulated scenarios, in €/L. Circular points represent the obtained P50 for each case, while the lower and higher boundaries of the boxes represent the P10 and P90 for each case, respectively. The shaded blue area represents the projected price of synthetic fuel production in 2050.

Table 11. Probability of the Simulated Cases Producing Jet Fuel Within the Projected Price

	base	*recycle*	*recycle + reforming*
probability (case A/case B)	2.68%/2.68%	5.47%/48.59%	14.23%/40.33%

processes in the market. This approach is often called "system expansion by avoided burden" and translates a consequential or societal perspective of CCU systems.[50]

6.1. Product Focused Approach−Recycled Carbon Fuel Classification. *6.1.1. Methodology.* The functional unit for the product-based approach is 1 MJ of the lower heating value (LHV) of jet fuel.

The system boundaries are cradle-to-grave, including (1) life-cycle emissions of inputs, (2) processing emissions and wastes, and (3) jet fuel combustion in its end-use. It also covers emission savings related to the captured CO_2 that can be considered as an avoided emission until 2041, according to Part A's point 1 of the Annex of the Delegated Regulation (EU) 2023/1185.[48] This applies to all industrial plants in sectors covered by the EU Emission Trading System other than electricity generation. Product transport and distribution were excluded due to negligible impact compared to the combustion emissions that are calculated following the methodology proposed by the EU methodology,[48] assuming the "kerosene-type jet fuel" classification.

Primary data are mostly based on the process modeling and simulations described in Section 2, whereas background data for the life cycle inventory associated with the flows interacting with the foreground system are obtained from Ecoinvent databases v3.8 and literature. Particularly, the supply chain of electricity was adapted to match the consumption mix for Portugal in the year of 2021, based on data by the Directorate General for Energy and Geology.[51,52] More details on the inventory data, assumptions, and databases selected are found in Supporting Information.

A major difference compared to the 14040:2006[49] and the Global CO_2 Initiative[50] methodology for LCA, used in Section 6.2, is that infrastructure impacts are not accounted for, which leads to the consideration that the emissions associated with renewable energy sources like wind and solar PV and renewable H_2 are considered to be zero. Accordingly, the carbon intensity of the electricity grid was determined following the methodology outlined in Part C of the same Annex,[48] yielding a value of 27.2 gCO2eq/MJ, considerably lower than the 67.3 gCO2eq/MJ obtained for the same electricity mix using Ecoinvent libraries v3.8.

In terms of the multifunctionality approach used, since all products are fuels and heat, an energy allocation is employed. System impacts are therefore apportioned among the different products according to their LHV, as shown in Figure 9 for the three cases.

The characterization factors for the Global Warming Potential (GWP-100*y*) according to the Renewable Energy Directive are from IPCC Assessment Report 4 (2007). However, in this study, the most updated characterization

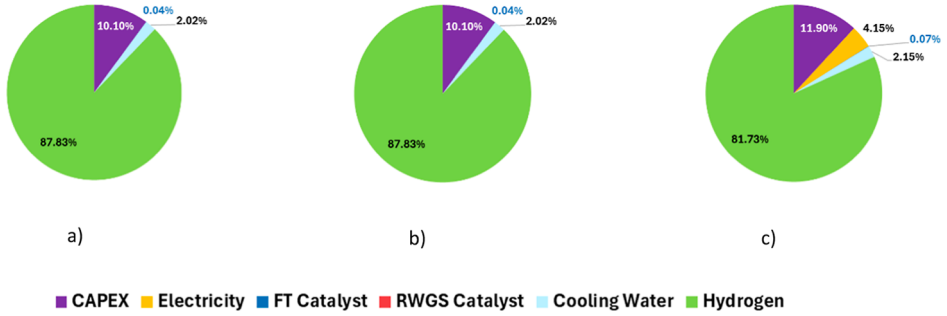

Figure 6. Cost Distribution for (a) *Base* Case; (b) *Recycle* Case; and (c) *Recycle + Reforming* Case, using the P50 for each variable and a H_2 Price of 2€/kg.

https://doi.org/10.1021/acs.iecr.5c03132
Ind. Eng. Chem. Res. 2025, 64, 22321−22335

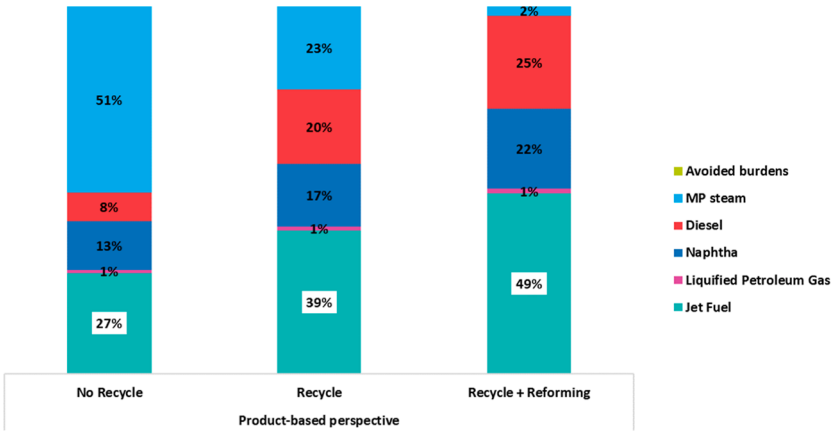

Figure 7. Partitioning of the Fischer–Tropsch process impacts among products for each scenario under the energy allocation approach.

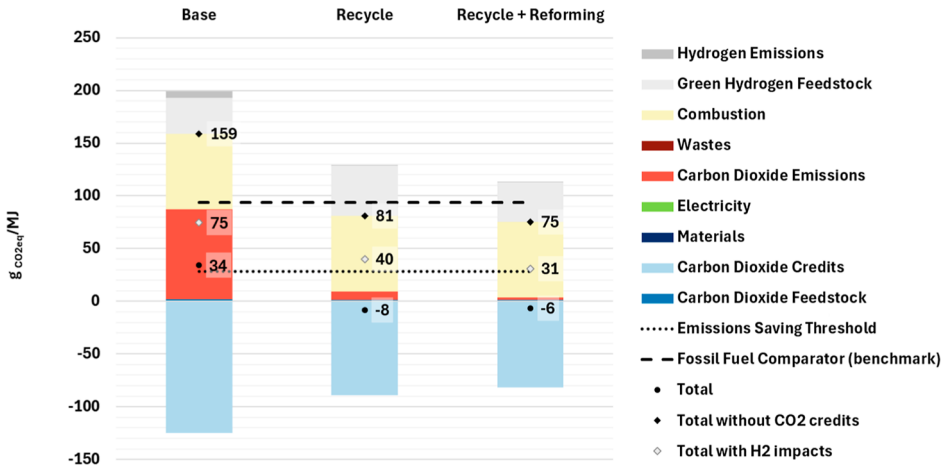

Figure 8. Global Warming Potential (100*y*) impacts in gCO_2eq per MJ of jet fuel produced in each scenario resulting from the application of the EU methodology.

factors according to the Sixth Assessment Report of the Intergovernmental Panel on Climate Change (IPCC),[14] as recommended by the International LCA Guidelines proposed by the EU Joint Research Centre.[53,54] This is also used in system expansion.

6.1.2. Results. The GWP impacts of jet fuel produced in each FT scenario are shown in Figure 10. The "Total" result represents the sum of all the impact contributions considered in the EU methodology up to and including 2040, namely, the feedstocks and materials in blue shades, the energy use in green, the processing emissions and wastes in red shades, and the final jet fuel combustion in yellow. "Carbon Dioxide Feed" includes the electricity, steam and materials consumption of the CO_2 capture process at the glass plant. "Materials" contains the consumption of catalysts and MEA of the FT process. "Green Hydrogen Feed", which contains the renewable energy hybrid plant and the electrolyzer infrastructure, and "Hydrogen Air Emissions" from the FT process, are not part of the "Total" and "Total without CO_2 credits" results that are compared with the benchmark of 94 gCO2eq/MJ and the emission saving threshold of 28.2 gCO2eq/MJ.

It is worth noting that, in this case, the steam required for CO_2 capture ("Carbon Dioxide Feed") was assumed to be generated using an electric boiler. This choice was motivated by efforts to improve the process performance, as steam production using a gas boiler was previously found to contribute significantly to the overall global warming potential (GWP), particularly in the *Recycle* and *Recycle + Reforming* scenarios. Under that assumption, all scenarios exceeded the GWP threshold for classifying jet fuel as a sustainable, recycled carbon fuel (28.2 gCO_2/MJ). The corresponding results and analysis are presented in the Supporting Information.

When using the electric boiler, the GWP impacts are significantly reduced compared with the results in Figure S4. The *Base* case achieves emission savings of 64% compared to the benchmark, but these are insufficient to achieve the threshold. In contrast, both alternative scenarios comply with the emission-saving criteria by achieving more than a 70% reduction, as they even achieve net negative carbon footprints, with the avoided emissions at the glass plant being larger than the additional CCU emissions and combustion emissions together.

These results indicate that the low carbon footprint associated with the Portuguese electricity grid makes the use of the electric boiler an effective measure to ensure the two proposed jet fuel production scenarios would meet the GHG savings criteria until 2041.

Further CO_2 capture improvements by using novel and more efficient separation methods could yet be explored to improve the performance even further. However, despite any potential further improvement, CO_2 credits are indispensable to offset combustion emissions. Without considering the CO_2

https://doi.org/10.1021/acs.iecr.5c03132
Ind. Eng. Chem. Res. 2025, 64, 22321−22335

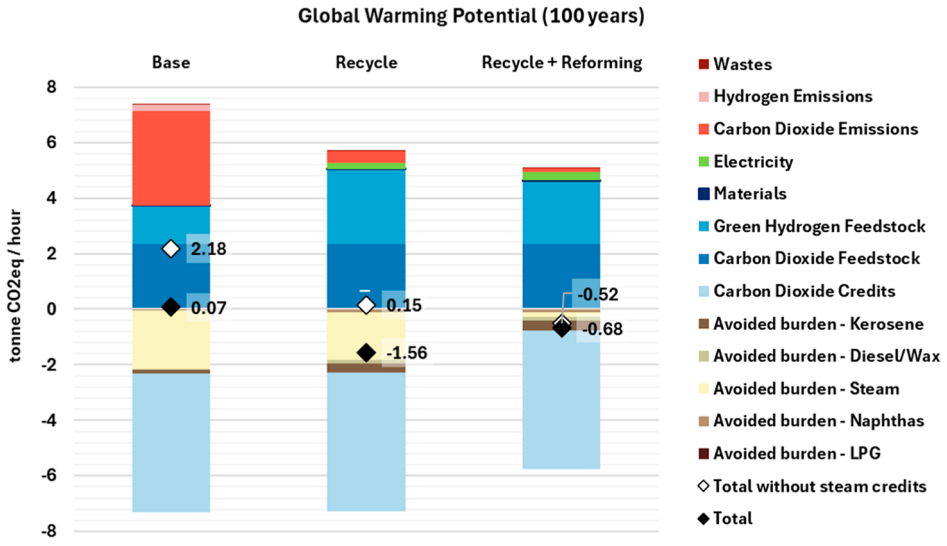

Figure 9. Global Warming Potential (100 years) impacts for each FT scenario under a system expansion approach.

credits, the GWP is 81 and 75 gCO_2/MJ, for *Recycle* and *Recycle + Reforming*. While these values remain below the fossil fuel benchmark of 94 gCO_2/MJ, they exceed the threshold required. This means that from 2041 onward, the jet fuel produced in these two scenarios would not comply with the established European requirements to be classified as a recycled carbon fuel, unless the CO_2 used comes from another sustainable source, such as sustainable biomass feedstocks or waste.

The gray shades in Figure 8 represent GWP contributors that are excluded from this analysis according to the EU methodology: the H_2 feed and the H_2 emissions from the FT plant. In the *Recycle* and *Recycle + Reforming* scenarios, processing H_2 emissions are reduced from 6 to less than 1 gCO_2/MJ, but this benefit is residual compared to the effect caused by the increase of H_2 requirements, which raises its specific impact by 41% and 9%, respectively. This constitutes a trade-off brought by the two proposed jet fuel production scenarios that is "silenced" with this methodology.

Furthermore, the inclusion of these contributors would significantly increase jet fuel GWP as observed in the "Total with H_2 impacts" results. In the studied scenarios, the production of green H_2 has a carbon footprint ranging from 34 to 47 gCO_2/MJ of jet fuel across scenarios, being larger than the emission saving threshold alone. This is a major vulnerability associated with the EU methodology, particularly to support the comparison between two alternative processes differing in terms of H_2 requirements.

6.2. Market Focused Approach. *6.2.1. Methodology.* The functional unit used to assess the marginal effects is 1 operational hour of the CCU system, easily translated into the reference flows of the produced jet fuel and other coproducts.

System boundaries follow a cradle-to-gate approach, including (1) raw materials extraction, processing, and distribution for all material and energy inputs, (2) processing emissions and wastes, and (3) credits stemming from the displaced use of conventional products. Product transport, distribution, and final use are not considered since considerable differences between CCU-based products and conventional products are not expected.

The unit processes included in the foreground system are the CO_2 capture from the flue gas, the jet fuel plant (Figure 2), the H_2O electrolysis, and the displaced processes, such as the conventional production of kerosene.

In this method, infrastructure is included in the primary data—solar PV and wind hybrid power plant for the electrolyzer infrastructure are based on literature[55,56] and the results from the optimization model[43] are used to size the plant—and in the background data, particularly that associated with the electricity supply chain, which considers the same mix used in the product-focused, but it is modeled using Ecoinvent database 3.8. Infrastructure for the CO_2 capture plant and jet fuel plant was not included in the inventory. Considering the benefits of using an electric boiler for CO_2 capture from flue gas discussed in the previous section, this approach focuses exclusively on the electric boiler option. The modeling of the displaced processes is based on the Ecoinvent database v3.8.

The multifunctionality of the FT process is solved by indirectly integrating all of the products into the functional unit.

For the impact assessment, the ReCiPe (H) 2016 V1.06 midpoint characterization method is used. It comprises 18 impact categories, but only some of the most critical categories related to energy transition technologies are herein analyzed, being Global Warming Potential (GWP-100*y*), with updated characterization factors according to the sixth Assessment Report of the IPCC;[14] Mineral Resources Scarcity (MRS); Fossil Resources Scarcity (FRS); and Water Consumption (WC). In addition, a GWP-100*y* factor for atmospheric H_2 emissions of 5 kg CO_2eq per kg H_2 was considered according to Derwent et al.[57]

6.2.2. Results. The GWP results of the three scenarios are listed in Figure 9. The "Total" results from the sum of all the impact contributions of the jet fuel plant—the feedstocks and materials in blue shades, the energy use in green, the processing emissions and wastes in red—and the avoided burdens resulting from the substitution of conventional processes in brown shades. A climate mitigation potential is thus expressed by a negative "Total" result, whereas a positive value indicates an increase in emissions compared to the benchmark market processes.

Despite the use of renewable energy sources for producing H_2 and the avoidance of 5 tons of CO_2 per hour, the *Base* case results in a larger GWP than the conventional processes, i.e.,

https://doi.org/10.1021/acs.iecr.5c03132
Ind. Eng. Chem. Res. 2025, 64, 22321−22335

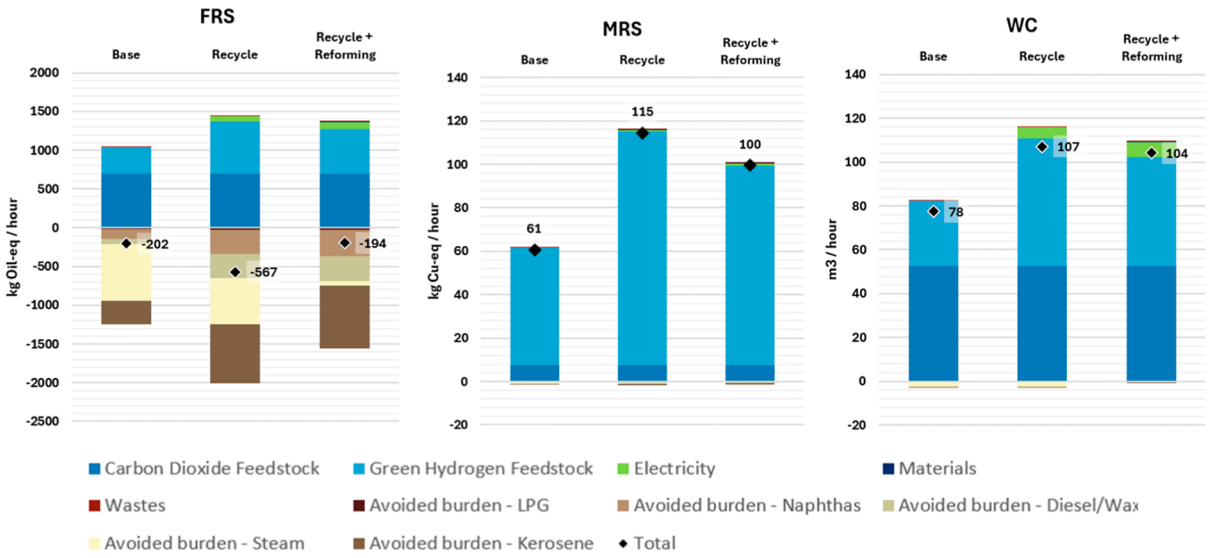

Figure 10. Results for the Fossil Resources Scarcity (FRS), Mineral Resources Scarcity (MRS) and Water Consumption (WC) impacts for each FT scenario under the system expansion approach.

the emission of flue gas and fossil-fuel-based FT operation. This means that their substitution with the proposed CCU system would result in an increase in emissions of about 70 kg of CO_2 per hour. The 3.36 tons of CO_2 direct emissions are the main contributor to this impact (46%), followed by the indirect emissions related to the flue gas CO_2 capture (32%) and green H_2 production (19%).

The process modifications tested in the *Recycle* and *Recycle + Reforming* scenarios lead to an abrupt reduction of process direct emissions. As shown in Figure 9, despite the increased demand for green H_2, the overall performance improves. The CCU system implementation would achieve a reduction of 1.56 and 0.68 tons of CO_2eq per hour for the *Recycle* and the *Recycle + Reforming*, respectively. It is worth noting that these benefits are only realized if all products from the jet fuel production plant substitute their conventional counterparts, and it is dependent on how the displaced products are modeled. Among all products, steam shows the greatest variability in associated environmental impacts across scenarios, as its substitution potential is more influenced by surrounding operations and their temporal elasticity toward steam needs. In a more conservative analysis, where the steam does not lead to any avoided burden ("Total without steam credits"), only the *Recycle + Reforming* scenario leads to a reduction in emissions of about 0.52 tons of CO_2eq per hour.

The process proposed in the *Recycle + Reforming* scenario results in the lowest emissions when avoided burdens are not considered (0.08 tons of CO_2eq per hour). Carbon and green H_2 feeds are the main contributors, followed by electricity used. The use of renewables-powered electricity and the improvement of the CO_2 capture process performance with other novel and more efficient separation methods compared to the benchmark herein modeled (i.e., MEA absorption) could, therefore, constitute effective measures to reduce emissions even further.

None of the proposed CCU systems would constitute a positive climate mitigation strategy if the CO_2 captured were not considered an avoided emission, a situation that could figure in the long term when other decarbonization technologies become feasible, such as direct or indirect electrification or the use of biogases.

For the other impacts, Figure 10 shows that the proposed scenarios achieve a net reduction in the consumption of fossil fuels (FRS) but also increase the pressure on the scarcity of mineral resources (MRS) and water (WC).

MRS is mainly associated with the infrastructure. The results obtained are mainly driven by the green H_2 demand across scenarios, corresponding to about 61 kg Cu-eq/hour for the *Base* case and 100 to 115 kg of Cu-eq/hour for the alternative scenarios, which benefit from higher jet fuel productivity and net GWP reductions.

WC is mainly driven by H_2O electrolysis and water H_2O makeup in CO_2 capture. Thus, the increased green H_2 demand in the *Recycle* (107 m^3/h) and *Recycle + Reforming* (104 m^3/h) scenarios worsens the impact associated with the *Base* case (78 m^3/h). These impacts are particularly critical for regions facing increasingly more severe drought situations, such as Portugal.[58] Alternatives such as recycling wastewater and desalination, as proposed by Simões et al.,[59] and its effect on the overall process performance should be explored.

The displacement of the conventional production pathways offsets all FRS impacts that arise mainly from energy use in the CO_2 capture and the supply chain related to the infrastructure required to produce green H_2. The result for the *Recycle* scenario (−567 kg Oil-eq/hour) is lower than for the *Base* case (−202 kg Oil-eq/hour), suggesting the effect of decreasing steam production due to the CO_2 recycling loop is compensated by the higher jet fuel productivity. The same does not occur in the *Recycle + Reforming* scenario, but it still achieves a net reduction of the 194 kg Oil-eq/hour.

7. CONCLUSIONS

This study evaluated the techno-economic and environmental performance of the CO_2 capture from a flue gas stream and its conversion to jet fuel, via reverse water gas shift followed by Fischer−Tropsch synthesis, considering three operational scenarios: (1) a *Base* scenario, where no recycle streams are considered, (2) a *Recycle* scenario where unreacted CO_2 and H_2 are recycled, and (3) *Recycle + Reforming* where, in addition to recycling part of the CO_2 and H_2, a reforming step is

https://doi.org/10.1021/acs.iecr.5c03132
Ind. Eng. Chem. Res. 2025, 64, 22321−22335

employed to generate some additional H_2 to be fed back to the FT reactor.

The introduction of recycling streams and reforming stages had a clear benefit in terms of the carbon efficiency of the process, which increased from 30% in the *Base* scenario to 85 and 91% in the *Recycle* and *Recycle + Reforming* scenarios. Despite leading to a larger demand on electricity and generating less steam per volume of fuel produced, the introduction of the recycle and reforming stages tripled the production of jet fuel, and the amount of diesel increased 60%. Comparing the *Recycle* and *Recycle + Reforming* scenarios, the latter has a specific consumption of fresh H_2 23% lower than that of the *Recycle* case, producing significantly less steam.

A stochastic analysis of the production costs showed the *Base* scenario has less than 3% probability of reaching the projected synthetic fuel price, comprehended between 1.16 and 2.55 €/L. For alternative scenarios, this probability rises to 40% if byproduct revenues from steam, electricity, diesel, LPG, and naphtha are considered. The *Recycle + Reforming* scenario is less dependent on byproduct revenues, compared to the *Recycle* scenario, with the probability of remaining in the projected range dropping to 14% versus 5.5%. This is the main advantage of this scenario, stemming from the reduced need for fresh H_2, which is the main contributor to the costs.

The environmental performance was assessed in a 2-fold approach. In a product-focused assessment, it was found that, unlike the *Base* case, jet fuel produced under the *Recycle* and *Recycle + Reforming* scenarios could be classified as a Recycled Carbon Fuel under EU regulation, though only until 2041. Beyond this point, more sustainable, nonfossil carbon sources must be adopted to ensure that emissions are genuinely avoided and eligible for carbon credit issuance. The performance of the CO_2 capture process was identified as a key contributor to the impact. Specifically, assuming steam generation via an electric boiler significantly reduced the GWP, enabling both alternative scenarios to meet the emission reduction threshold. In this configuration, avoided emissions exceeded the direct and indirect emissions from the CCU processes, resulting in net-negative carbon footprints: −8 gCO_2eq/MJ for *Recycle* and − 6 gCO_2eq/MJ for *Recycle + Reforming*.

The market-focused assessment revealed that, in contrast to the *Base* case, capturing CO_2 from the flue gas and displacing conventional production of kerosene, diesel, LPG, and steam through the CCU systems in the *Recycle* and *Recycle + Reforming* scenarios led to systemic life-cycle GHG reductions of −1.56 and −0.68 tonnes of CO_2eq per hour, respectively. This demonstrates the net benefit of reducing direct process emissions and increasing Fischer−Tropsch productivity via the recycle loop despite the higher H_2 demand. All proposed CCU systems also reduced FRS but increased MRS and WC, particularly in the *Recycle* scenario (115 kg Cu-eq/h and 107 m^3/h) and *Recycle + Reforming* (100 kg Cu-eq/h and 104 m^3/h). Besides the reduced trade-offs, the *Recycle + Reforming* scenario showed lower dependency on the effective displacement of coproducts, especially steam, which is highly sensitive to local conditions.

Green H_2 was a major contributor to all impact categories, including GWP. This highlights a key vulnerability in the EU methodology: the inclusion of indirect emissions from H_2 production not only prevents achieving the 70% emissions savings threshold but also biases comparisons between processes with differing H_2 requirements.

Given that both alternative scenarios enable jet fuel classification as a Recycled Carbon Fuel until 2041, the choice between them depends largely on the opportunity to displace conventional steam production. In such cases, the *Recycle* scenario offers greater reductions in systemic GWP, FRS, and production costs, albeit with higher WC and MRS.

However, there were also some limitations inherent to the different simulations. First, solely the Atmospheric Crude Distillation Unit was simulated, which is the first step of crude processing within a refinery. This limits the product quality, as neither product is ready to sell. Furthermore, the inclusion of subsequent steps, such as hydrocracking, may enhance the jet fuel yield. Additionally, the possibility of obtaining CO_2 and/or H_2 as a byproduct from other industries may decrease the feedstock price, thus increasing the economic feasibility of the process.

■ ASSOCIATED CONTENT

Supporting Information

The Supporting Information is available free of charge at https://pubs.acs.org/doi/10.1021/acs.iecr.5c03132.

(i) Simulation basis and assumptions, (ii) Aspen flowsheets; (iii) H2 model outputs; (iv) the used Life-Cycle Inventory (LCI) and (v) the GHG estimations, according to the Delegated Acts on Renewable Fuels of Non-Biological Origin (PDF)

■ AUTHOR INFORMATION

Corresponding Author

Fernando G. Martins − *LEPABE, ALiCE, Faculty of Engineering, University of Porto, Porto 4200-465, Portugal;* orcid.org/0000-0003-0960-4620; Email: fgm@fe.up.pt

Authors

Marcelino Artur L. Fernandes − *CoLAB NET4CO2, Porto 4200-355, Portugal*

Frederico S. Coelho − *CoLAB NET4CO2, Porto 4200-355, Portugal*

Rita M. Martinho − *CoLAB NET4CO2, Porto 4200-355, Portugal; CENSE − Centre for Environmental and Sustainability Research Energy and Climate, NOVA School of Science and Technology, NOVA University Lisbon, Almada 2829-516, Portugal*

Mariana G. Domingos − *CoLAB NET4CO2, Porto 4200-355, Portugal; STAR Institute - Science & Technology Applied Research, Lugar do Pombal, Zona Industrial do Salgueiro, Viseu 3530-259, Portugal*

Complete contact information is available at: https://pubs.acs.org/10.1021/acs.iecr.5c03132

Notes

The authors declare no competing financial interest.

■ ACKNOWLEDGMENTS

This work was financially supported by the funding program under the Recovery and Resilience Plan (Missão Interface N.° 01/C05-i02/2022 and Missão Interface N.° 03/C05-i02/2022) and by national funds through FCT/MCTES (PIDDAC): LEPABE, UIDB/00511/2020 (DOI: 10.54499/UIDB/00511/2020), UIDP/00511/2020 (DOI: 10.54499/UIDP/00511/2020), and ALiCE, LA/P/0045/2020 (DOI: 10.54499/LA/P/0045/2020).

REFERENCES

(1) Worldometer Oil. https://www.worldometers.info/oil/(accessed November 2023).
(2) Agency, I. E. *Growth in Global Oil Demand is Set to Slow Significantly by 2028*. https://www.iea.org/news/growth-in-global-oil-demand-is-set-to-slow-significantly-by-2028 (accessed Jan 2024).
(3) *T&E E-fuel Cars are Not Zero Emission*. https://www.transportenvironment.org/articles/e-fuel-cars-are-not-zero-emission (accessed Oct 2024).
(4) Commission, E. *Union Registry*. https://climate.ec.europa.eu/eu-action/eu-emissions-trading-system-eu-ets/union-registry_en (accessed Jun 2024).
(5) Agency, I. E. *CO2 Capture and Utilisation*. https://www.iea.org/energy-system/carbon-capture-utilisation-and-storage/co2-capture-and-utilisation (accessed Jun 2024).
(6) Commission, E. ReFuelEU Aviation. https://transport.ec.europa.eu/transport-modes/air/environment/refueleu-aviation_en#:~:text=ReFuelEU%20Aviation%20promotes%20the%20increased,target%20of%2055%25%20by%202030%20 (accessed Mar 2025).
(7) Insights, F. B. *Methanol Market to Exhibit 4.5% CAGR till 2028; Replacement of Heavy Fuels with Methyl Alcohol in Marine Industry to Drive Growth Globally*. https://www.fortunebusinessinsights.com/press-release/global-methanol-market-10130 (accessed Aug 2024).
(8) market.*Us Jet Fuel Oil Market*. https://market.us/report/jet-fuel-oil-market/(accessed Aug 2024).
(9) market.*Us Dimethyl Ether Market*. https://market.us/report/dimethyl-ether-market/(accessed Aug 2024).
(10) Zhang, C.; Gao, R.; Jun, K.-W.; Kim, S. K.; Hwang, S.-M.; Park, H.-G.; Guan, G. Direct conversion of carbon dioxide to liquid fuels and synthetic natural gas using renewable power: Techno-economic analysis. *J. CO2 Util* **2019**, *34*, 293−302.
(11) Colelli, L.; Segneri, V.; Bassano, C.; Vilardi, G. E-fuels, technical and economic analysis of the production of synthetic kerosene precursor as sustainable aviation fuel. *Energy Convers. Manage.* **2023**, *288*, 117165.
(12) Gao, R.; Zhang, C.; Jun, K.-W.; Kim, S. K.; Park, H.-G.; Zhao, T.; Wang, L.; Wan, H.; Guan, G. Transformation of CO2 into liquid fuels and synthetic natural gas using green hydrogen: A comparative analysis. *Fuel* **2021**, *291*, 120111.
(13) Gao, R.; Zhang, C.; Jun, K.-W.; Kim, S. K.; Park, H.-G.; Zhao, T.; Wang, L.; Wan, H.; Guan, G. Green liquid fuel and synthetic natural gas production via CO2 hydrogenation combined with reverse water-gas-shift and Co-based Fischer−Tropsch synthesis. *J. CO2 Util* **2021**, *51*, 101619.
(14) IPCC, *I. P. O. C. C. Climate Change 2023 - Synthesis Report*. https://www.ipcc.ch/report/ar6/syr/downloads/report/IPCC_AR6_SYR_FullVolume.pdf (accessed Nov 2024).
(15) Kirsch, H.; Sommer, U.; Pfeifer, P.; Dittmeyer, R. Power-to-fuel conversion based on reverse water-gas-shift, Fischer−Tropsch Synthesis and Hydrocracking: Mathematical modeling and simulation in Matlab/Simulink. *Chem. Eng. Sci.* **2020**, *227*, 115930.
(16) Comidy, L. J. F.; Staples, M. D.; Barrett, S. R. H. Technical, economic, and environmental assessment of liquid fuel production on aircraft carriers. *Appl. Energy* **2019**, *256*, 113810.
(17) Zhang, Y.; Li, A.; Fei, Y.; Zhang, C.; Zhu, L.; Huang, Z. Techno-economic assessment of electro-synthetic fuel based on solid oxide electrolysis cell coupled with Fischer−Tropsch strategy. *J. CO2 Util* **2024**, *86*, 102905.
(18) Adelung, S.; Dietrich, R.-U. Impact of the reverse water-gas shift operating conditions on the Power-to-Liquid fuel production cost. *Fuel* **2022**, *317*, 123440.
(19) Freire Ordóñez, D.; Halfdanarson, T.; Ganzer, C.; Shah, N.; Dowell, N. M.; Guillén-Gosálbez, G. Evaluation of the potential use of e-fuels in the European aviation sector: a comprehensive economic and environmental assessment including externalities. *Sustain. Energy Fuels* **2022**, *6* (20), 4749−4764.
(20) Schemme, S.; Breuer, J. L.; Köller, M.; Meschede, S.; Walman, F.; Samsun, R. C.; Peters, R.; Stolten, D. H2-based synthetic fuels: A techno-economic comparison of alcohol, ether and hydrocarbon production. *Int. J. Hydrogen Energy* **2020**, *45* (8), 5395−5414.
(21) Delgado, H. E.; Cappello, V.; Zang, G.; Sun, P.; Ng, C.; Vyawahare, P.; Elgowainy, A. A.; Wendt, D. S.; Boardman, R. D.; Marcinkoski, J. Techno-economic analysis and life cycle analysis of e-fuel production using nuclear energy. *J. CO2 Util* **2023**, *72*, 102481.
(22) Dieterich, V.; Buttler, A.; Hanel, A.; Spliethoff, H.; Fendt, S. Power-to-liquid via synthesis of methanol, DME or Fischer−Tropsch-fuels: a review. *Energy Environ. Sci.* **2020**, *13* (10), 3207−3252.
(23) Mahouri, S.; Catalan, L. J. J.; Rezaei, E. Process design and techno-economic analysis of CO2 reformation to synthetic crude oil using H2 produced by decomposition of CH4 in a molten media. *Energy Convers. Manage.* **2023**, *276*, 116548.
(24) Markowitsch, C.; Lehner, M.; Maly, M. Evaluation of process structures and reactor technologies of an integrated power-to-liquid plant at a cement factory. *J. CO2 Util* **2023**, *70*, 102449.
(25) Wang, W.-C.; Liu, Y.-C.; Nugroho, R. A. A. Techno-economic analysis of renewable jet fuel production: The comparison between Fischer−Tropsch synthesis and pyrolysis. *Energy* **2022**, *239*, 121970.
(26) Weyand, J.; Habermeyer, F.; Dietrich, R.-U. Process design analysis of a hybrid power-and-biomass-to-liquid process − An approach combining life cycle and techno-economic assessment. *Fuel* **2023**, *342*, 127763.
(27) Mivechian, A.; Pakizeh, M. Hydrogen recovery from Tehran refinery off-gas using pressure swing adsorption, gas absorption and membrane separation technologies: Simulation and economic evaluation. *Korean J. Chem. Eng.* **2013**, *30* (4), 937−948.
(28) Luo, X.; Hartono, A.; Hussain, S.; Svendsen, H. Mass transfer and kinetics of carbon dioxide absorption into loaded aqueous monoethanolamine solutions. *Chem. Eng. Sci.* **2015**, *123*, 57−69.
(29) Rangel, G. P.; Domingos, M. G.; Lopes, J. C. B.; Neto, B. Sustainable green hydrogen production: Trading off costs and environmental impacts. *Int. J. Hydrogen Energy* **2025**, *100*, 994−1009.
(30) Vidal Vázquez, F.; Pfeifer, P.; Lehtonen, J.; Piermartini, P.; Simell, P.; Alopaeus, V. Catalyst Screening and Kinetic Modeling for CO Production by High Pressure and Temperature Reverse Water Gas Shift for Fischer−Tropsch Applications. *Ind. Eng. Chem. Res.* **2017**, *56*, 13262−13272.
(31) Ghogia, A. C.; Nzihou, A.; Serp, P.; Soulantica, K.; Pham Minh, D. Cobalt catalysts on carbon-based materials for Fischer−Tropsch synthesis: a review. *Appl. Catal., A* **2021**, *609*, 117906.
(32) Pandey, U.; Runningen, A.; Gavrilović, L.; Jørgensen, E. A.; Putta, K. R.; Rout, K. R.; Rytter, E.; Blekkan, E. A.; Hillestad, M. Modeling Fischer−Tropsch kinetics and product distribution over a cobalt catalyst. *AIChE J.* **2021**, *67* (7), No. e17234.
(33) Serge-Bertrand, A.; Rifat Radisovich, M., Crude Distillation Unit (CDU). In *Anal. Chem.*, Abhay Nanda, S., Ed. IntechOpen: Rijeka, 2020; p Ch. *6*.
(34) Dincer, I.; Rosen, M. A.; Al-Zareer, M. 3.11 Chemical Energy Production. In *Comprehensive Energy Systems*; Dincer, I., Ed.; Elsevier: Oxford, 2018; pp 470−520.
(35) Matthey, J. *Guide to approach-to-equilibrium*. https://matthey.com/documents/161599/441284/JM+Guide+to+ATE+flier+(c2020)+.pdf/77700e80-2ca4-0c9e-3a34-738a2145168f?t=1653488896115 (accessed Jul 2024).
(36) Okoye-Chine, C. G.; Moyo, M.; Liu, X.; Hildebrandt, D. A critical review of the impact of water on cobalt-based catalysts in Fischer−Tropsch synthesis. *Fuel Process. Technol.* **2019**, *192*, 105−129.
(37) Zang, G.; Sun, P.; Elgowainy, A.; Bafana, A.; Wang, M. Q. Performance and cost analysis of liquid fuel production from H2 and CO2 based on the Fischer−Tropsch process. *J. CO2 Util* **2021**, *46*, 101459.
(38) BusinessAnalytiq Monoethanolamine price index. https://businessanalytiq.com/procurementanalytics/index/monoethanolamine-price-index/(accessed Mar 2024).
(39) *Statista Average Monthly Electricity Wholesale Price in Portugal from January 2019 to September 2024*. https://www.statista.com/

https://doi.org/10.1021/acs.iecr.5c03132
Ind. Eng. Chem. Res. 2025, 64, 22321−22335

statistics/1281464/portugal-monthly-wholesale-electricity-price/(accessed Mar 2024).
(40) *Statista Futures Price of Cobalt Worldwide from August 2019 to August 2023*. https://www.statista.com/statistics/1171975/global-monthly-price-of-cobalt/(accessed Mar 2024).
(41) *Statista Average Nickel Prices from 1980 to 2022*. https://www.statista.com/statistics/236578/iron-ore-prices-since-2003/(accessed Mar 2024).
(42) *Statista Monthly Price of Naphtha Worldwide from January 2020 to December 2022*. https://www.statista.com/statistics/1318098/monthly-price-naphtha-worldwide/(accessed Mar 2024).
(43) Gustavo, P. R.; Domingos, M. G.; Lopes, J. C. B.; Neto, B. *Sustainable Green Hydrogen Production: Trading off Costs and Environmental Impacts*; Elsevier 2024.pp994−1009
(44) Mylpg.eu Chart of fuel prices in Portugal. https://www.mylpg.eu/stations/portugal/prices (accessed Oct 2024).
(45) TLV Calculator: Steam Unit Cost. https://toolbox.tlv.com/global/TI/calculator/steam-unit-cost.html?advanced=on (accessed Mar 2024).
(46) *Oracle Crystal Ball*. https://www.oracle.com/applications/crystalball/(accessed Jan 2024).
(47) Powerfuels, G. A. Powerfuels in Aviation. https://www.dena.de/fileadmin/dena/Publikationen/PDFs/2019/Powerfuels_in_Aviation_GAP.pdf (accessed Jul 2024).
(48) Commission, E. *Commission Delegated Regulation Supplementing Directive (EU) 2018/2001 of the European Parliament and of the Council by Establishing a Minimum Threshold for Greenhouse Gas Emissions Savings of Recycled Carbon Fuels and by Specifying a Methodology for Assessing Greenhouse Gas Emissions Savings from Renewable Liquid and Gaseous Transport Fuels of Non-biological Origin and from Recycled Carbon Fuels*; In C(2023) 1086: Brussels, 2023.
(49) ISO 14044 *Environmental Management - Life Cycle Assessment - Requirements and Guidelines*; 2006.
(50) Langhorst, T., McCord, S., Zimmerman, A., Muller, L., Cremonese, L., Strunge, T., Wang, Y., Zaragoza, A. V., Wunderlich, J., Marxen, A., Armstrong, K., Buchner, G., Katelhon, A., Bachmann, M., Sternberg, A., Michailos, S., Naims, H., Winter, B., Rosckosch, D., Faber, G., Mangin, C., Mason, F., Stokes, G., Williams, E., Olfe-Krautlein, B., Styring, P., Schomacker, R., Bardow, A., Sick, V., *Techno-Economic Assessment & Life Cycle Assessment Guidelines for CO2 Utilization (Version 2)*; 2022.
(51) Geologia, D. G. E. e. *ProduçA∼O Anual E PotêNcia Instalada - Disponibilidade De Energia ElétRica Para Consumo*. https://www.dgeg.gov.pt/pt/estatistica/energia/eletricidade/producao-anual-e-potencia-instalada/(accessed Mar 2024).
(52) Geologia, D. G. E. e. *ImportaçO∼Es De GáS Natural Anuais 2000−2020P*. https://www.dgeg.gov.pt/pt/estatistica/energia/gas-natural/importacoes-exportacoes/(accessed Mar 2024).
(53) *ILCD Recommendations for Life Cycle Impact Assessment in the European Context - Based on Existing Environmental Impact Assessment Models and Factors*.; European Union: Luxemburg, 2011.
(54) *ILCD General Guide for Life Cycle Assessment - Detailed Guidance*. https://eplca.jrc.ec.europa.eu/uploads/ILCD-Handbook-General-guide-for-LCA-DETAILED-GUIDANCE-12March2010-ISBN-fin-v1.0-EN.pdf (accessed May 2024).
(55) Bareiß, K.; de la Rua, C.; Möckl, M.; Hamacher, T. Life cycle assessment of hydrogen from proton exchange membrane water electrolysis in future energy systems. *Appl. Energy* **2019**, *237*, 862−872.
(56) Wulf, C.; Reuß, M.; Grube, T.; Zapp, P.; Robinius, M.; Hake, J.-F.; Stolten, D. Life Cycle Assessment of hydrogen transport and distribution options. *J. Clean. Prod* **2018**, *199*, 431−443.
(57) Derwent, R. G.; Stevenson, D. S.; Utembe, S. R.; Jenkin, M. E.; Khan, A. H.; Shallcross, D. E. Global modelling studies of hydrogen and its isotopomers using STOCHEM-CRI: Likely radiative forcing consequences of a future hydrogen economy. *Int. J. Hydrogen Energy* **2020**, *45*, 9211−9221.
(58) Soares, P. M. M.; Dias, L.; Lemos, G.; Bento, V.; Lima, D.; Antunes, C.; C, R.; M, E.; Ferreira, V.; S, M.; Catita, C.; I, B.; Costa, P.; Dacamara, C.; Nunes, S.; Cardoso, R.; Santos, L.; P, C.; M, S.; Bushenkova, A., *National Roadmap for Adaptation 2100: Portuguese Territorial Climate Change Vulnerability Assessment for XXI Century − Report WP7: Regional Adaptation Storylines*. 2024.
(59) Simoes, S. G.; Catarino, J.; Picado, A.; Lopes, T. F.; di Berardino, S.; Amorim, F.; Gírio, F.; Rangel, C. M.; Ponce de Leão, T. Water availability and water usage solutions for electrolysis in hydrogen production. *J. Clean. Prod* **2021**, *315*, 128124.

https://doi.org/10.1021/acs.iecr.5c03132
Ind. Eng. Chem. Res. 2025, 64, 22321−22335